

## Artificially ordered FeCu alloy superlattices on Cu(001). II. Spin-resolved electronic properties and magnetic dichroism

W. Kuch, M. Salvietti, Xingyu Gao, M.-T. Lin,\* M. Klaua, J. Barthel, Ch. V. Mohan, and J. Kirschner  
Max-Planck-Institut für Mikrostrukturphysik, Weinberg 2, D-06120 Halle, Germany

(Received 24 February 1998)

Spin-resolved electronic and element-resolved magnetic properties of artificial fcc FeCu alloy thin films, grown epitaxially by pulsed-laser deposition in the ordered  $L1_0$  phase on Cu(001), were studied by spin-resolved valence-band photoemission and soft x-ray circular magnetic dichroism. Valence-band photoemission reveals bands which are present due to the reduced periodicity of the layered alloy films. Dichroism measurements attest that the Fe atoms in FeCu are all ferromagnetic, and carry magnetic moments similar to those of ultrathin fcc Fe films on Cu(001). The Fe orbital moments are found to be significantly enhanced with respect to pure Fe, with an orbital to spin moment ratio of  $\approx 0.12$ . An increase in the number of Cu 3d holes in the FeCu films as well as induced Cu  $d$  moments are observed, which amount to  $\approx 0.11 \mu_B$ .

[S0163-1829(98)03537-1]

### I. INTRODUCTION

The characterization of magnetic alloys with respect to their magnetic and electronic properties merits great attention both because of fundamental interest and because of having, via the composition, an additional adjustable parameter for tailoring materials with technologically desired properties. Chemically ordered phases of magnetic alloys can be stabilized by ferromagnetism,<sup>1</sup> and may exhibit magnetic properties which differ significantly with respect to the disordered phase.<sup>2</sup> In ultrathin films the situation is even more complex due to the occurrence of substrate-induced strain and the enhancement of magnetic anisotropies.<sup>3</sup> Since fcc Fe ultrathin films have turned out to be one of the most complex and thus most widely studied systems in thin-film magnetism,<sup>4</sup> magnetic alloys containing fcc Fe are especially fascinating with respect to the interplay of electronic, structural, and magnetic properties. FeCo and FeNi ultrathin alloy films can be stabilized in the fcc phase over a wide range of compositions when grown on Cu(100).<sup>5,6</sup> The magnetic characterization of these two Fe-based alloy systems has already revealed interesting magnetic phenomena: In FeCo a switching of the magnetic easy axis from in-plane to out-of-plane as a function of composition occurs;<sup>7</sup> FeNi films exhibit an unusual behavior of the Curie temperature with film thickness.<sup>6</sup>

Little is known, in contrast, of the electronic and magnetic properties of FeCu ultrathin films. Artificial alloys of these otherwise immiscible elements have been synthesized mechanically in the bulk by ball-milling techniques<sup>8-11</sup> and sputtering.<sup>12,13</sup> It was reported that for Fe concentrations below  $\approx 70\%$  the fcc structure is assumed, and for higher Fe concentrations the bcc structure is assumed.<sup>10,13</sup> This was confirmed by an extended x-ray fine structure analysis of these artificial FeCu bulk alloys.<sup>11</sup> Magnetic measurements pointed towards the segregation of nonferromagnetic fcc  $\gamma$ -Fe at elevated temperatures,<sup>14,15</sup> whereas the Fe atoms in the fcc FeCu alloy exhibited ferromagnetic moments greater than  $2\mu_B$  for Fe concentrations of 50% and higher,<sup>9,10,12-14</sup>

in accordance with theory,<sup>16</sup> ruling out the presence of a nonferromagnetic fcc Fe phase. A recent calculation for disordered fcc FeCu alloys yielded nonferromagnetic fcc iron only for more than 80% Fe content, and about constant Fe moments for lower Fe concentrations.<sup>17</sup>

In magnetic multilayers in which ultrathin Cu layers are sandwiched between ferromagnetic layers, and also in CoCu alloys it has been observed that small magnetic moments are induced in the Cu atoms by the vicinity of the magnetic atoms. Cu  $d$ -band moments of  $0.05\mu_B$  in Co/Cu multilayers,<sup>18,19</sup>  $0.14\mu_B$  (Ref. 18) and  $0.12\mu_B$  (Ref. 19) in  $\text{Co}_{90}\text{Cu}_{10}$ , as well as  $sp$ -band moments of  $-0.02\mu_B$  (Ref. 20) have been determined. Theoretical calculations affirmed this finding, yielding moments for the interfacial Cu atoms in Co/Cu multilayers of  $0.02\mu_B$ ,<sup>21</sup>  $0.03\mu_B$ ,<sup>22</sup>  $0.05\mu_B$  for the spin moment with contributions of  $0.07$  ( $-0.02$ )  $\mu_B$  from  $d$  ( $p$ ) states,<sup>23</sup> and  $0.05\mu_B$  from  $d$  states and  $-0.03\mu_B$  from  $sp$  states.<sup>18</sup> For Fe/Cu multilayers Cu induced moments of  $0.07\mu_B$ ,<sup>21</sup>  $0.05\mu_B$ ,<sup>22</sup> and  $0.06\mu_B$  (Ref. 24) have been calculated. For a layered FeCu alloy the resulting theoretical moment was  $0.08\mu_B$ .<sup>24</sup> An experiment on Fe/Cu multilayers gave a total  $d$ -shell moment of up to  $0.09\mu_B$ , depending on the Cu layer thickness.<sup>19</sup>  $K$ -edge circular magnetic dichroism data on Fe/Cu multilayers indicated a negative contribution of the  $p$ -band moment to the induced Cu moment, but no quantitative conclusion was drawn.<sup>20</sup> To our knowledge no experimental investigations of Cu magnetic properties in FeCu alloys exist up to date.

In this contribution we report spin-resolved electronic and element-resolved magnetic properties of Fe and Cu in artificially layered FeCu alloys, prepared epitaxially by pulsed-laser deposition on Cu(001).<sup>25,26</sup> The FeCu films hereby exist as an ordered fcc alloy of the  $L1_0$  type, consisting of alternately deposited atomic layers of (001) oriented fcc Fe and Cu. The method of depositing successively single atomic layers of different materials to produce artificial layered alloys has been already employed for the fabrication of FeAu and FePt alloys.<sup>27</sup> It is very important to grow the single atomic layers as flat and smooth as possible in order to ob-

tain the desired order in the alloy thin film. For FeCu on Cu(001) pulsed-laser deposition has to be employed, because it is known that thermal evaporation of Fe on Cu(001) causes islanding and the simultaneous growth of the first two atomic layers.<sup>28</sup> Details of the deposition and the structural characterization of the films can be found in Ref. 26.

We present measurements of spin-resolved ultraviolet photoemission spectroscopy (SPUPS), and magnetic circular dichroism in soft x-ray absorption (XMCD). With SPUPS the occupied spin-split magnetic band structure of ferromagnetic metals and alloys can be probed,<sup>29</sup> as was shown for FeCo ultrathin alloy films on Cu(001).<sup>30</sup> XMCD as a complementary technique probes the spin asymmetry of the unoccupied part of the band structure just above the Fermi level.<sup>31</sup> The magnetic dichroism is caused by transitions of spin-polarized core-level electrons, excited by circularly polarized x rays, into the unoccupied part of the exchange split valence bands. The dichroism, i.e., the intensity difference upon reversal of either the light helicity or the magnetization direction, is a consequence of the different transition probabilities for spin-up and spin-down electrons into the mainly minority-type unoccupied bands. Sum rules have been proposed to deduce quantitative information from XMCD spectra.<sup>32,33</sup> Although there has been some dispute about the applicability of these rules,<sup>34–37</sup> they seem to yield reasonable results for the  $3d$  transition metals.<sup>36–40</sup> One feature of the sum rules is that under some assumptions they allow to deduce quantitative information about the number of unoccupied states, as well as the spin and orbital moments from comparing the absorption cross section at the  $L_2$  and  $L_3$  edges of transition metals.<sup>32,33,41</sup>

The remainder of this paper is organized as follows: The experimental details are described in the following section. In Sec. III we present the results of the SPUPS measurements. Section IV contains the results of the XMCD measurements, divided into measurements at the Fe- $L_{2,3}$  (Sec. IV A) and Cu- $L_{2,3}$  edge (Sec. IV B). In Sec. V we summarize our findings.

## II. EXPERIMENT

For the present study films of 10 and 22 atomic layers (monolayers, ML), alternatingly consisting of Fe and Cu, were deposited by pulsed-laser deposition on a Cu(001) substrate. The details of the film preparation are described in Ref. 26. The films grow in a layer-by-layer mode already starting with the first layer, as judged by reflection high-energy electron diffraction (RHEED) during growth. Capping layers were evaporated on top of the films for protection against residual gases: For the samples used in the SPUPS experiments one additional ML of Cu was deposited on top of the terminating Cu layer, and for the XMCD measurements the films were capped with 3 ML of Au in order to avoid dilution of the Cu elemental information from FeCu by a Cu cap layer.

After preparation of the samples, which was done at the laboratory in Halle, the samples were transferred under ultrahigh vacuum (UHV) conditions to the Berlin synchrotron radiation source (BESSY). During the transport ( $\approx 170$  km) a pressure of about  $4 \times 10^{-8}$  Pa was maintained in the transfer chamber. The typical time interval for transfer and trans-

port elapsed between the preparation of the samples and the beginning of the measurements at BESSY was about 4 h.

Reference Fe/Co films were grown on Cu(001) *in situ* by electron beam evaporation from high-purity Fe and Co rods. Typical evaporation rates were here 1–2 min/ML. The growth mode and deposition rate were monitored during evaporation by RHEED. No contamination within the Auger electron spectroscopy limit ( $\approx 1\%$ ) could be detected after deposition.

All of the experiments described in this paper were conducted at a sample temperature of 120 K. Prior to the photoemission or -absorption measurements the magnetization of the films along the in-plane  $[110]$  direction was checked using longitudinal magneto-optical Kerr effect (MOKE). At all of the samples square hysteresis loops could be observed. The measurements were performed in remanence, the presence of which was regularly checked between and after scans of data acquisition. The direction of the magnetization was switched by ramping the magnetic field with the same coil which was also used for the MOKE measurements.

Different UHV chambers at different beamlines of BESSY were used for the SPUPS and XMCD measurements. The base pressure in both chambers was  $1 \times 10^{-8}$  Pa. Spin-resolved photoemission spectra were taken at the 6.5 m normal-incidence monochromator beamline, which offers circularly polarized light in the vacuum ultraviolet region.<sup>42</sup> The spectra presented in this paper were taken for normal incidence of the incoming radiation, and normal emission of the outgoing photoelectrons. The circular polarization of the exciting radiation is thereby irrelevant for the component of the spin-polarization along the magnetization direction due to the high experimental symmetry, and spectra for both helicities were averaged. The sample magnetization was reversed each  $\approx 40$  min of acquisition time. The total time for the acquisition of one spin-resolved spectrum at a certain photon energy presented here was typically 6 h.

The electron spectrometer is described in detail elsewhere.<sup>43</sup> It allows the detection of normally emitted electrons for normal incidence of the incoming radiation. For the measurements presented in this paper it was operated at a fixed pass energy of 8 eV, resulting in an overall energy resolution of approximately 200 meV (including the monochromator resolution). The angular acceptance can be estimated to be less than  $\pm 2^\circ$ . After passing the energy analyzer the photoelectrons are accelerated to 104 eV kinetic energy, and diffracted at a W(001) surface. The spin information is then obtained from the intensities of the elastic  $\langle 02 \rangle$  diffraction spots, which are recorded with a two-stage channelplate.<sup>43</sup>

XMCD experiments were performed at the PM-3 (SX-700 III) beamline at BESSY. This beamline is constructed to offer circularly polarized soft x-ray radiation by selecting light from above or below the orbital plane of the electrons in the storage ring. For the measurements presented here the acceptance was set to be 0.3 mrad below the ring orbit, which should produce a circular polarization of nominally 65%.<sup>44</sup> In practice, however, the resulting degree of polarization is lower and not exactly known. By comparing the measured magnetic moments of a thick Co reference film using sum rules to the literature value of  $1.64\mu_B$  the authors of Ref. 45 concluded a value of 48% for an equivalent setting

of the same beamline. Own measurements of Co reference films, analyzed as described below, yielded an estimate of about 40% for the degree of circular polarization. This value will be used in the following. It should be mentioned that the results, as far as absolute values of magnetic moments are concerned, may thus be subject to a certain systematic error. Comparing moments obtained from different samples under identical conditions, however, should yield more reliable quantities.

The monochromator exit slit was set to 50  $\mu\text{m}$ , resulting in an energetic resolution of  $\approx 1.5$  eV in the region of the Fe and Cu  $L$  edges. The angle of incidence of the sample was chosen to be  $45^\circ$ , which represents a compromise between a high circular dichroism, and the minimization of saturation effects which occur due to the finite penetration depth of the exciting radiation in the resonant absorption maximum.<sup>46</sup> For the present geometry and the film thicknesses considered here we estimate these saturation effects to introduce an maximum error of 2%. The total electron yield of the sample was recorded by measuring the drain current with a bias voltage of  $-27$  V applied. The spectra were normalized to the current of a gold grid monitor located just behind the monochromator exit slit. The analysis of the spectra was done as outlined in Refs. 36 or 41. In particular, the spectra were normalized to unity edge jump. Subsequently, a background consisting of two step functions of 0.5 eV width and statistical heights of 2/3 and 1/3 at the positions of the  $L_3$  and  $L_2$  absorption maxima, respectively, was subtracted from the Fe spectra in order to obtain the Fe  $L_{2,3}$  white line intensity. A constant number of Fe  $3d$  holes of 3.34 was assumed,<sup>34</sup> rather than determining the constant ratio between the white line intensity and the number of holes from a sample with a known moment.<sup>41</sup> The Cu  $L$ -edge spectra were analyzed by comparing them to the spectra of Ref. 18, taking into account the different angle of incidence and the different degree of light polarization in our experiment. In this way it is not necessary to independently determine the number of Cu  $3d$  electrons in the FeCu alloys. Instead, the value for the ratio of white line intensity to number of  $d$  holes for Cu of Ref. 18 is taken, which is assumed to be transferable for a given element.<sup>41</sup>

### III. SPIN-RESOLVED VALENCE-BAND PHOTOEMISSION

Spin-resolved photoemission spectra of a 10 ML FeCu film on Cu(001), taken in normal emission for normal light incidence, are presented in Fig. 1 for various photon energies ranging from 12 to 22 eV. A peak between 2 and 3 eV binding energy  $E_B$  can be seen, accompanied by a broad plateau towards lower binding energies. Except for  $E_B < 1$  eV a prevailing majority spin-polarization is found. Comparing the spectra to those of ultrathin fcc Fe films on Cu(001),<sup>30,47</sup> the peak at 2–3 eV can be assumed to be mainly derived from Cu  $3d$  states, and the plateau at 0–2 eV from Fe  $3d$  states. The spectra of Fig. 1 differ from the spin-resolved spectra found for Fe on Cu(001) (Ref. 30) in that the peak is broader, and the plateau is more flat, in the sense that the intensity does not rise towards the Fermi energy  $E_F$ , as it does for Fe/Cu(001).<sup>30</sup> The Fe-derived signal in the plateau shows a lower relative intensity with respect to the Cu derived peak than in pure Fe films, which is consis-

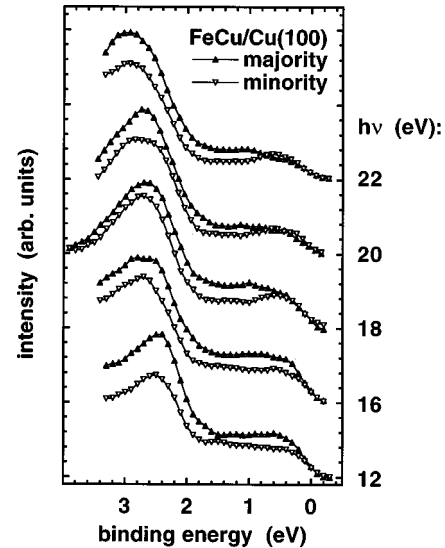


FIG. 1. Spin-resolved photoemission spectra of 10 ML FeCu/Cu(001) for various photon energies  $h\nu$ , taken in normal emission for normal light incidence. Filled (open) triangles denote majority-(minority-) spin spectra.

tent with the damping of the Cu substrate photoelectrons in Fe/Cu(001), and with emission from the additional Cu cap layer on top of the FeCu film. A dispersing minority peak is seen for photon energies above 18 eV at binding energies between 0 and 0.5 eV, which probably shifts above the Fermi level for lower  $h\nu$ . At 12 and 16 eV photon energy an increase of the minority emission in the plateau towards higher binding energies is observed, whereas at higher photon energies it is constant except for the previously mentioned peak near  $E_F$ . The Cu-derived signal at 2–3 eV binding energy appears with a similar shape in both the majority and the minority partial spectra. No significant spin polarization in this peak can thus be concluded from the present spectra.

Upon varying the photon energy for normal electron emission only the electron momentum component perpendicular to the film plane  $k_\perp$  is varied. The presence of a dispersion with photon energy, and hence with  $k_\perp$ , which becomes obvious from Fig. 1, shows that the artificial layered alloy films develop a three-dimensional volume band structure. If there was no hybridization of electronic states between the single Fe and Cu layers, a two-dimensional behavior of the electronic states within the layers and thus no dispersion with photon energy would be expected, which is not the case.

The rather broad structures of the spectra of Fig. 1 do not allow a precise determination of band positions. More information can be gained from plotting the spin polarization, defined as the difference between the partial intensity spectra for majority and minority spin normalized to the total intensity. This is done in Fig. 2, where the spin polarization corresponding to the spectra of Fig. 1 is depicted. The minority emission near  $E_F$  for photon energies above 18 eV shows up as local minimum in the spin-polarization curves. In addition, two prominent maxima are observed in each curve, which are traced in Fig. 2 by dotted lines. These maxima may be interpreted as energetic positions of majority spin

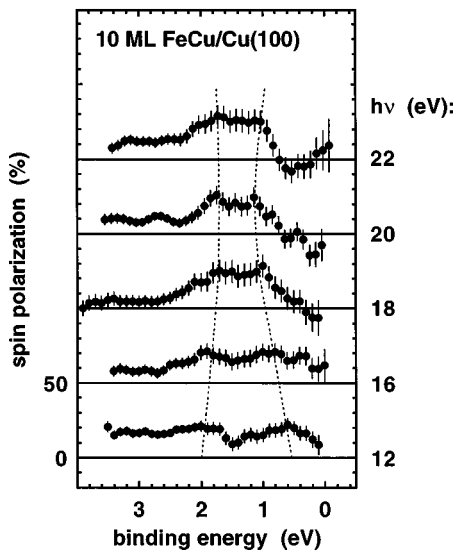


FIG. 2. Spin polarization, defined as difference between majority and minority photoemission intensity normalized to the total intensity, of the spectra of Fig. 1. The dotted lines point out the dispersion of two positive maxima.

type bands with mainly Fe character. Their dispersion with photon energy would then reflect the dispersion of these bands along the  $\Delta$  axis in  $k$  space, i.e., for zero parallel component  $k_{\parallel}$  of the electron momentum vector.

The energetic positions of the positive maxima of Fig. 2 are plotted in Fig. 3 versus  $k_{\perp}$ . To determine the  $k_{\perp}$  values, free-electron-like parabolas were assumed for the final-state bands with an inner potential of 7.5 eV with respect to  $E_F$ . The full range of the  $x$  axis in Fig. 3,  $2\pi/a$ , corresponds to the distance from  $\Gamma$  to  $X$  in the simple fcc lattice with perpendicular lattice parameter  $a$ . In the layered FeCu structures the  $x$ -axis range is twice that distance, and  $X$  is in the center. The dispersion of the positive polarization maxima in that

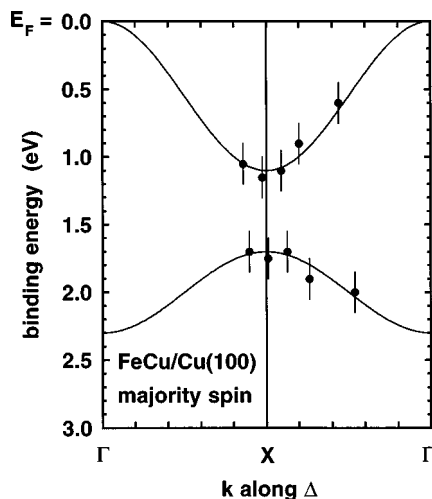


FIG. 3. Energetic positions of the positive maxima of Fig. 2 plotted over the perpendicular component of the electron momentum. The  $x$  axis is labeled according to the reduced zone scheme in the layered FeCu alloys due to the doubled periodicity perpendicular to the film plane. The solid lines are guides to the eye; they illustrate the interpretation in terms of Fe-derived majority bands.

reduced zone scheme is consistent with a dispersion of Fe-derived bands. The solid curves in Fig. 3 are guides to the eye, and suggest how the bands may be interpreted. In the case of pure fcc Fe there is a majority band of  $\Delta^5$  spatial symmetry, which contributes to the spectra in our geometry.<sup>30</sup> According to band-structure calculations it starts at the  $X$  point at the Fermi edge, and disperses down to about 2.4 eV at  $\Gamma$ .<sup>48</sup> The zone center is crossed at  $\approx 1.3$  eV. An FeCu band derived from that Fe band would show a similar dispersion if plotted as a function of the absolute value of  $k_{\perp}$ , regardless of the zone boundaries. In Fig. 3 that would mean that this Fe band would start at  $E_F$  at the left side, and end at 2.4 eV at the right side. However, considering the reduced zone in the layered FeCu alloys due to the doubled periodicity perpendicular to the film plane an additional back-folded band should be present which shows exactly the opposite dispersion. The solid lines in Fig. 3 indicate such a behavior. At the “new”  $X$  point of the FeCu Brillouin zone, where these bands would cross each other, the degeneracy of the crossing is lifted, and the bands split off to form a gap. Identifying the experimental polarization maxima with band positions, the band gap at the  $X$  point of the reduced FeCu zone is located between 1.2 and 1.7 eV binding energy.

The minority emission which is observed around 0.5 eV binding energy for  $h\nu = 18\text{--}22$  eV, i.e., around  $X$  of the FeCu zone, is probably related to the exchange split counterpart of the lower branch of the majority band. At lower photon energies, where one would expect a downward dispersion towards  $\Gamma$ , it is probably masked by the emission from the upper branch of the majority bands. If we attributed the binding energy of 0.5 eV, at which the minority feature is observed, directly to a band position, an exchange splitting of only 1.2 eV would result. The high-spin phase of fcc Fe though is expected to show an average exchange splitting of more than 2 eV.<sup>48,49</sup> This seeming discrepancy could be due to the fact that the minority emission is cut off by the Fermi edge, in such a way that the observed structure in the minority spectra just represents the shoulder of the actual peak, which is located above  $E_F$ . Also conceivable is that the gap at  $X$  generated by the lifted degeneracy of the two branches could be different for the minority-type bands, leading to a different exchange splitting of the upper and lower branches at the  $X$  point.

A similar dispersion as for the Fe-derived bands may be expected for bands derived from the corresponding Cu 3d states. In pure Cu, these bands disperse from  $E_B \approx 2$  eV at  $X$  to about 3.5 eV at  $\Gamma$ .<sup>47,50</sup> It is difficult to extract experimental band positions of the FeCu bands derived from these states from the present spectra of Fig. 1 because of the large width of the peak around 2.5–3 eV. This width could be attributed to the simultaneous emission from the second, lower branch, contributing to the intensity in the shoulder towards higher binding energy. Assuming the same inner potential of 7.5 eV as before, a photon energy of 22 eV would correspond to  $k_{\perp}$  at about the  $X$  point of the FeCu Brillouin zone. At this photon energy the Cu-derived peak is located at  $E_B \approx 3$  eV, which is the same binding energy as has been found at the center of the Brillouin zone of pure Cu.<sup>47</sup> Taking this as a hint for a similar dispersion as a function of absolute  $k_{\perp}$  values in FeCu and Cu, there must be some overlap between the lower branch of the Fe-type majority band, and the upper

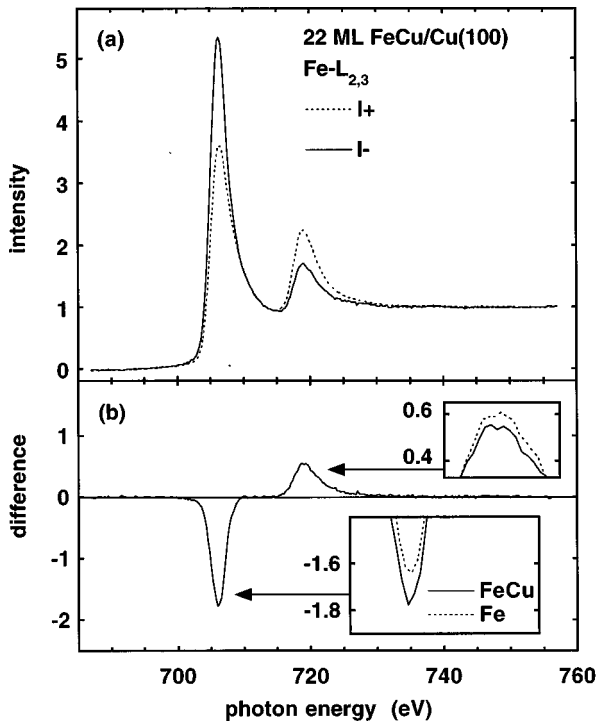


FIG. 4. (a) Absorption spectra at the Fe- $L_{2,3}$  edge of a 22 ML film of FeCu for parallel (solid lines) and antiparallel alignment of magnetization direction and light helicity (dotted lines). The spectra have been corrected for the angle of light incidence and the estimated degree of circular polarization. (b) Difference between the spectra of (a). The insets show blowups of the  $L_2$  and  $L_3$  edges, comparing the absorption difference of the FeCu film (solid lines) to that of a 3.5 ML fcc Fe reference film (dotted lines).

branch of the Cu-type band near  $\Gamma$  at  $\approx 2.2$  eV binding energy. Hybridization of these bands might consequently be expected, leading to a certain extent of spin polarization of the Cu derived bands. It is this kind of hybridization between spin-split bands of Fe  $3d$  type with bands of mainly Cu  $3d$  character, which can be expected also at other points in  $k$  space, that leads to the interesting question how these electronic hybridizations might affect the magnetic properties of the FeCu films, and in particular the magnetic moments on the Fe and Cu atoms in the alloy.

#### IV. SOFT X-RAY MAGNETIC DICHROISM

##### A. Fe- $L_{2,3}$ edge

Absorption spectra at the Fe- $L_{2,3}$  edge of a 22 ML film of FeCu are shown in Fig. 4(a). Spectra for parallel and antiparallel alignment of magnetization direction and light helicity are reproduced by solid and dotted lines, respectively. The spectra are corrected for the angle of light incidence, and the estimated degree of circular polarization (cf. Sec. II). The difference between the two spectra is plotted in Fig. 4(b). Already at first glance it can be stated that the strong dichroism is comparable in size to published XMCD data of bcc Fe (Refs. 36, 37, 40) and fcc Fe,<sup>40,51</sup> and to that observed at reference Fe films. The insets of Fig. 4(b) show blowups of the  $L_2$  and  $L_3$  edges, comparing the absorption difference of the FeCu film (solid lines) to that of a 3.5 ML fcc Fe reference film (dotted lines). The latter was grown on a 5 ML Co

buffer layer on Cu(001). The Co buffer layer is necessary to align the easy axis of magnetization, which would be perpendicular in the case of 3.5 ML Fe/Cu(001),<sup>4,52</sup> to the film plane,<sup>53</sup> thus assuring identical experimental conditions as for the FeCu alloy films. Although the overall spectral shape of the FeCu and Fe difference spectra is very similar, distinct differences are observed right at the absorption edges. Pure Fe shows a smaller dichroism at the  $L_3$  edge, and a higher dichroism at the  $L_2$  edge than does FeCu.

A more precise analysis of the data is achieved by the means of sum rules,<sup>32,33</sup> which link the integrated intensity differences at the  $L_2$  and  $L_3$  edges, corrected for the incomplete degree of circular polarization and the angle of incidence, to the atomic orbital and spin moments. According to the first sum rule, the orbital moment is proportional to the integral over both the  $L_2$  and  $L_3$  edges,<sup>32</sup> i.e., the difference of the (positive) areas of the dichroism at the  $L_3$  and  $L_2$  maxima. Even without a quantitative analysis it follows immediately that the orbital moment of the Fe atoms is larger in FeCu than in the Fe reference film.

The second sum rule builds a connection between the absolute dichroism, integrated separately at the  $L_2$  and  $L_3$  edges, and the spin magnetic moment.<sup>33</sup> The sum of the (positive) areas of the dichroism at the  $L_3$  edge and twice the dichroism at the  $L_2$  edge is proportional to the spin moment, plus a term describing a dipolar interaction.<sup>33</sup> The latter is thought to be small for  $3d$  metals,<sup>33,54</sup> and is often neglected.<sup>36-40</sup> In both sum rules the results are normalized to the integrated white-line intensity.

Fe atomic moments for 10 and 22 ML FeCu alloy films on Cu(001) and the 3.5 ML fcc Fe film, obtained from applying the sum rules to the XMCD spectra and neglecting the dipole term, are given in the respective rows of Table I. The Fe spin moments  $\mu_S$  show no significant difference between the two FeCu films and the Fe film, considering the accuracy of the analysis (about  $\pm 5\%$ ). The white-line intensity, which is proportional to the number of  $d$ -band holes, remains also constant within this error. No significant change in the number of Fe  $3d$  electrons can thus be concluded from our data. The similarity in the observed Fe moments between FeCu and Fe rules out the presence of nonferromagnetic fcc Fe in the alloy films, as it was supposed for FeCu bulk samples at elevated temperatures.<sup>14,15</sup> All three values of the Fe spin moment  $\mu_S$  are slightly lower than the Fe bulk moment ( $2.1 \mu_B$ ).<sup>55</sup> This might be due to systematic errors connected to the very details of the steplike background subtracted for white-line integration, the exact degree of circular polarization, or the number of  $3d$  holes.

The Fe orbital moments  $\mu_L$  of the FeCu films, in contrast to the spin moments, are significantly enhanced with respect to the Fe sample. Note that the ratio  $\mu_L/\mu_S$ , given in the last column of Table I, is insensitive to the assumptions made for the degree of circular polarization and the number of  $3d$  holes.

Increased orbital moments have been observed previously for decreasing thickness of Co overlayers on Cu(001),<sup>56</sup> in Co/Pd multilayers,<sup>57,58</sup> Co/Pt multilayers,<sup>57</sup> and in Fe/Pd multilayers.<sup>39</sup> They are interpreted in terms of the reduced coordination at the surface or at the interface, leading to a higher density of states at the Fermi level, which in turn results in enhanced orbital moments.<sup>56,59</sup> In the FeCu alloy

TABLE I. Spin ( $\mu_S$ ) and orbital magnetic moments ( $\mu_L$ ) of Fe and Cu atoms in FeCu/Cu(001) films from a sum-rule analysis of XMCD measurements, as well as their ratio  $\mu_L/\mu_S$ . For comparison the result of a 3.5 ML Fe film on 5 ML Co/Cu(001), and literature values for a random  $\text{Co}_{90}\text{Cu}_{10}$  alloy and an Fe/Cu multilayer are also listed.

Sample	Atom	$\mu_S$ ( $\mu_B$ )	$\mu_L$ ( $\mu_B$ )	$\mu_L/\mu_S$
10 ML FeCu	Fe	1.8	0.21(5)	0.12(3)
	Cu	0.05	0.006(3)	0.12(6)
	Cu (film only) <sup>a</sup>	0.12	0.014(7)	0.12(6)
22 ML FeCu	Fe	1.8	0.26(6)	0.13(3)
	Cu	0.08	0.004(2)	0.05(3)
	Cu (film only) <sup>a</sup>	0.11	0.005(3)	0.05(3)
3.5 ML Fe/5 ML Co	Fe	1.9	0.08(2)	0.04
200 Å $\text{Co}_{90}\text{Cu}_{10}$ <sup>b</sup>	Cu	0.114 <sup>b</sup>	0.009 <sup>b</sup>	0.08 <sup>b</sup>
[10 Å Fe/3 Å Cu] <sub>20</sub> <sup>b</sup>	Cu	0.078 <sup>b</sup>	0.007 <sup>b</sup>	0.09 <sup>b</sup>

<sup>a</sup>Corrected to exclude the Cu substrate contribution, assuming an electron mean free escape depth of 11 ML ( $\approx 20$  Å).

<sup>b</sup>Reference 19.

films the reduction of symmetry along the surface normal could contribute to the enhancement of  $\mu_L$ . The results of Sec. III have shown that the electronic states of the ordered alloy films normal to the Fe and Cu planes are strongly modified with respect to the pure metal films. The observed orbital moments may thus be considered a consequence of the ordered layer stacking, and reflect the electronic structure of the FeCu films. The spin moments, on the other hand, are less sensitive to subtle changes of the electronic properties, which may explain that no significant differences in  $\mu_S$  between the fcc Fe and the FeCu films are observed.

Another point of view in the discussion of orbital moments is the connection to the magnetic anisotropy. The enhancement of  $\mu_L$  in Co/Pd and Co/Pt multilayers was interpreted in terms of an enhanced perpendicular anisotropy in these systems.<sup>57</sup> In a simple perturbation model the anisotropy of the orbital moment is linked to the magnetic anisotropy caused by spin-orbit coupling.<sup>60</sup> This leads to higher orbital moments in samples magnetized along the preferred magnetization axis compared to a magnetization direction forced along a hard axis by high magnetic fields,<sup>54,61</sup> and to a noncollinear orientation of spin and orbital moments in the latter case.<sup>62</sup> In the present study the XMCD measurements were performed in a fixed geometry (cf. Sec. II), with all samples magnetized remanently in the film plane. Fcc Fe films of 3.5 ML thickness on Cu(001) are known to show a perpendicular anisotropy,<sup>4,52</sup> and it has been found that Fe films exhibit very similar structural and magnetic properties when grown on thin Co/Cu(001) films rather than directly on Cu(001).<sup>53,63</sup> It is therefore very plausible that the intrinsic spin-orbit-derived anisotropy in the 3.5 ML fcc Fe/Co/Cu(001) sample is comparable to that of Fe/Cu(001), i.e., also perpendicular to the film plane. It could thus be that it is the additional anisotropy energy of the Co buffer layer which forces the magnetic easy axis of the Fe/Co bilayer system to be in-plane. A similar situation has been recently reported to occur in Co/Ni/Cu(001), where XMCD measurements in a transverse geometry have shown that a perpendicular magnetocrystalline anisotropy present in the Ni layer is overcome by the Co in-plane contribution to result in a common in-plane easy axis.<sup>64</sup> In the Fe/Co/Cu(001) system, according

to the above-mentioned connection between the magneto-crystalline anisotropy and the anisotropy of the orbital moment, this would lead to a lower  $\mu_L$  in the present geometry compared to a perpendicular magnetization direction. XMCD measurements of Fe films of comparable thicknesses of 3.4 and 3.8 ML, which were prepared directly on Cu(001) and measured with the magnetization along the surface normal, yielded indeed  $\mu_L/\mu_S$  ratios of about 0.07,<sup>40</sup> nearly twice as high as found here for the Fe/Co/Cu(001) film. We note that in Ref. 40 also significantly higher absolute values of both the spin moments  $\mu_S$  and orbital moments  $\mu_L$  have been obtained. As already pointed out though, the absolute values of both  $\mu_S$  and  $\mu_L$  may be subject to systematic errors, whereas the ratio  $\mu_L/\mu_S$  is less sensitive to the analysis procedure.

The orbital moments of the FeCu films are significantly higher than those predicted by theory. Calculations for one Fe monolayer in Cu(001),<sup>65</sup> and for an Fe/Cu monoatomic multilayer<sup>66</sup> resulted both in orbital moments of only  $\approx 0.07 \mu_B$ . Following the interpretation in terms of magnetic anisotropy the high orbital moments measured for in-plane magnetization of the FeCu films indicate a high in-plane anisotropy. This seems surprising at first glance, because for ultrathin fcc Fe films on Cu(001) there exist experimental<sup>4,52</sup> as well as theoretical<sup>67</sup> indications of a perpendicular anisotropy. For Fe monolayers sandwiched between Cu theoretical calculations resulted in a perpendicular anisotropy, too.<sup>65,67</sup> However, other calculations gave an in-plane anisotropy for fcc Fe films on Cu(001), and perpendicular anisotropy for Fe/Cu monoatomic multilayers.<sup>66</sup> Recent experimental investigations of ultrathin Fe/Cu(001), deposited by pulsed-laser deposition, revealed an in-plane orientation of the magnetic easy axis at thicknesses below 5 ML,<sup>68</sup> in contrast to thermally deposited Fe/Cu(001).<sup>4,52</sup>

Much of this contradiction may be related to the actual structure and atomic volume of the Fe films; the Fe films produced by pulsed-laser deposition in Ref. 68 exhibited significantly less tetragonal distortion than thermally deposited films. It is clear that in particular the vertical atomic distances of the Fe and Cu layers in the FeCu films will have a strong influence on the overlap and the hybridization be-

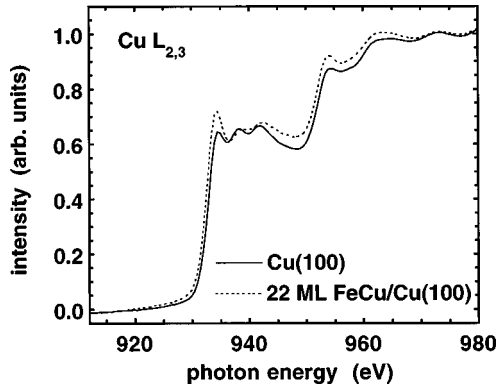


FIG. 5. Cu  $L_{2,3}$  absorption spectra of a 22 ML FeCu film, averaged over both magnetization directions (dotted line), and a clean Cu(001) sample (solid line).

tween Cu and Fe states, and hence on the electronic properties of the alloy film. We speculate that it is such subtle differences between the geometric structure assumed for the calculations and the actual structure realized in the pulsed-laser deposited alloy films which account for the differences in the orbital moment. The electronic structure is what basically determines both the magnetocrystalline anisotropy, and also the magnetic moments; the high orbital moments of the Fe atoms must thus be considered as reflecting the actual electronic structure of the FeCu(001) alloy films.

### B. Cu- $L_{2,3}$ edge

Information about the unoccupied electronic states at the Cu sites can be obtained from XMCD measurements at the Cu  $L_{2,3}$  edge. Figure 5 shows the absorption spectrum of a 22 ML FeCu(001) film, averaged over both magnetization directions (dotted line) together with the absorption spectrum of a clean Cu(001) surface (solid line). Several differences between the two curves are apparent. The most evident is the enhancement in intensity for the FeCu film right at the Cu  $L_3$  edge (934 eV photon energy). A smaller increase in intensity is also observed at the Cu  $L_2$  edge (954 eV). Since the  $L_{2,3}$  absorption intensity reflects the Cu unoccupied density of states above the Fermi edge, this can be judged as manifestation of an enhanced number of unoccupied Cu-like states in FeCu with respect to pure Cu metal. Theoretical calculations have shown that the absorption is mainly ( $\approx 95\%$ ) governed by transitions into  $d$ -like states.<sup>69</sup> The observed enhancement of the intensity at both the Cu  $L_3$  and  $L_2$  edges points thus towards an increase in the number of  $3d$  holes at the Cu atoms. This is probably directly related to the hybridization of  $3d$  bands with Cu and Fe character, as described in Sec. III.

Most of the additional unoccupied states are located just above the Fermi edge, because the strongest differences between the two curves of Fig. 5 are observed directly at the  $L_3$  and  $L_2$  edges. Similar enhancements of the Cu  $L_{2,3}$  absorption signal with respect to pure Cu can be seen in the spectra of  $\text{Co}_{90}\text{Cu}_{10}$  alloys or Fe/Cu multilayers presented in Refs. 18 and 19. Theoretical calculations for monoatomic Fe/Cu multilayers predict an opposite charge transfer of about 0.1 electron from Fe to Cu.<sup>24</sup> This calculated electron transfer is however mainly due to  $s$ - and  $p$ -like electrons,<sup>24</sup> whereas the  $2p \rightarrow 3d$  channel dominates the Cu  $L_{2,3}$  absorption.<sup>69</sup>

Differences between the spectra of Cu and FeCu of Fig. 5 are also observed in the  $L_3$  near-edge region. The two wiggles seen in the spectrum of clean Cu(001) at 738 and 741 eV photon energy are partially smeared out in the FeCu spectrum, and shifted towards higher photon energies. These wiggles can be attributed to singularities of the unoccupied density of states at the  $L$  and  $X$  points of the fcc Brillouin zone.<sup>69</sup> This fingerprint of a Cu fcc structure is, though modified, still observed in the FeCu spectrum. The results of Sec. III suggested that in the artificial FeCu alloy films periodic electronic states along the surface normal are formed which reflect the doubled periodicity in that direction. This will certainly also influence the unoccupied part of the band structure. Modifications and shifts of  $d$  bands due to hybridization at the new zone boundaries, as well as hybridization between Cu and Fe derived bands may account for the changes observed in the Cu  $L_3$  absorption spectrum.

The energetic shift of the post  $L_3$  edge wiggles towards higher energies may also be interpreted in terms of lattice parameter differences between FeCu and Fe. Assuming free-electron-like parabolic bands the observed shifts of about 0.5 eV would correspond to an  $\approx 2\%$  Brillouin-zone enlargement, or equivalently to a 2% reduction in lattice parameter. An anisotropic film lattice would consequently lead to a broadening of these features.

Discussing the shape of the Cu absorption spectra of FeCu/Cu(001) one has to keep in mind that even at 22 ML film thickness there is still a significant portion of substrate absorption measured by the total electron yield method. Assuming a mean electron escape depth of 11 ML ( $\approx 20$  Å), about 25% of the spectrum of the 22 ML FeCu film stems from absorption of Cu substrate atoms. Some of the remaining two-peak post-edge structure must therefore be attributed to the Cu substrate. Nevertheless, the basic observations are unaffected, as there are the increase in intensity at the energetic positions of the Cu  $L_2$  and  $L_3$  edges, and the broadening and shift of the absorption structures above the Cu  $L_3$  edge. They have to be attributed to modifications of the electronic structure. The structureless difference in absorption between 945 and 970 eV photon energy may either be also attributed to electronic effects upon alloying, or due to an extended absorption fine structure of Fe or the Au cap layer.

Figure 6 shows the magnetic dichroism at the Cu  $L_{2,3}$  edge. Presented are difference spectra of 10 and 22 ML FeCu/Cu(001) films in units of the Cu  $L_{2,3}$  edge jump height. Analogously to Fig. 4(b) the difference between absorption for antiparallel alignment of magnetization direction and light helicity, corrected for the angle of light incidence and the estimated degree of circular polarization, is depicted. The curve for 22 ML FeCu is vertically offset for clarity. A small but distinct dichroism at the energetic positions of the Cu  $L_3$  and  $L_2$  edges with the same sign as at the respective Fe edges is observed. It is larger for the 22 ML film, where it amounts to about  $-5\%$  and  $+2.5\%$  of the Cu  $L_{2,3}$  edge jump. A small magnetic moment is thus present at the Cu atoms, parallel to the Fe moment. The difference between the dichroism of the 10 and 22 ML films is explained by the contribution of unpolarized Cu substrate atoms, which is larger in the case of 10 ML FeCu.

The moments that are obtained by applying the sum rules to the spectra of Fig. 6 are listed in the second and fifth row

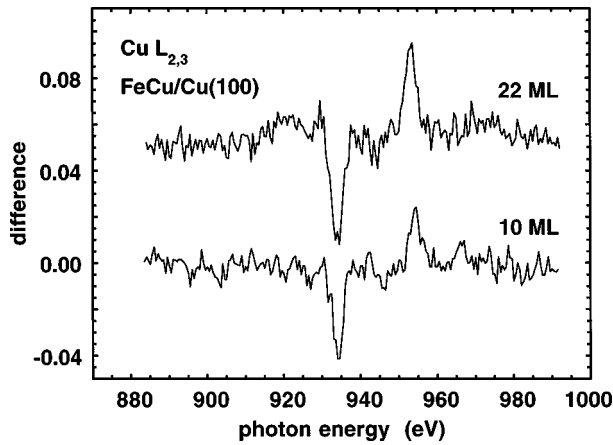


FIG. 6. Absorption difference between antiparallel and parallel alignment of magnetization direction and light helicity at the Cu  $L_{2,3}$  edge for FeCu/Cu(001) films of 10 and 22 ML thickness, corrected for the angle of light incidence and the estimated degree of circular polarization. The curve for 22 ML FeCu is offset for clarity.

of Table I. Other than in the analysis of the Fe spectra no integration of the Cu white-line intensity was performed. The dichroism spectra were instead compared to the ones presented in Refs. 18 and 19 (cf. Sec. II). The analysis of the data relies thereby on the proportionality factor of Refs. 18 and 19 between the number of  $d$  holes and the white-line intensity, which was derived from an extrapolation of bulk Fe, Co, and Ni factors to Cu.<sup>41</sup> This extrapolation may introduce a certain systematic error in the resulting moments. It has, on the other hand, the advantage that besides the difficult white-line integration also the assumption concerning the number of Cu  $3d$  holes becomes unnecessary.

As mentioned before, there is a substantial contribution of the Cu(001) substrate to the dichroism data. Assuming as before a mean information depth of 11 ML, about 25% of the signal of the 22 ML sample and about 55% of the signal of the 10 ML sample stem from Cu atoms of the substrate. Assuming further that none of the substrate atoms contributes to the magnetic dichroism, the corrected moments of the Cu atoms in the FeCu films are listed in the third and sixth row of Table I. (Counting the top atomic Cu layer of the substrate as a “film” layer would not change these numbers significantly.) Similar values for both the 10 and 22 ML films of  $0.12 \pm 0.01 \mu_B$  and  $0.11 \pm 0.007 \mu_B$ , respectively, are obtained for the Cu spin moments  $\mu_S$ . The cited errors hereby represent solely the accuracy of the experiment, and do not include systematic errors due to uncertainties of the analysis procedure. From the values of the corrected Cu moments it is seen that the different dichroism of the 10 and 22 ML FeCu films is indeed accounted for completely by the different attenuation of the substrate contribution.

In the bottom rows of Table I literature values for a random  $\text{Co}_{90}\text{Cu}_{10}$  alloy and an [Fe 10 Å/Cu 3 Å] multilayer from Ref. 19 are listed. The induced Cu  $3d$  spin moments of the ordered FeCu alloy films are comparable to the one reported for  $\text{Co}_{90}\text{Cu}_{10}$ , and about 50% larger than the one of the Fe/Cu multilayer. The latter are mainly (111) textured,<sup>19</sup> and the thickness of 3 Å of the Fe layers therein corresponds to about 1.5 ML. The difference in the induced moments

may thus be explained by, and would be consistent with, the different average chemical surroundings of the Fe atoms in our samples and in the Fe/Cu multilayers. In the ideal FeCu layered alloy each Cu atom is surrounded by four Cu nearest neighbors in the film plane, and eight Fe nearest neighbors above and below this film plane. In the Fe/Cu multilayer the Cu-Fe coordination is lower, on the one hand because of the (111) orientation (six nearest neighbors of the same species in the film plane), and on the other hand, because of the Fe layer thickness (1.5 ML compared to 1 ML, if considering the FeCu alloys as monoatomic multilayers). This certainly will reduce the overlap and the hybridization between Fe and Cu states, and hence the moments at the Cu sites.

On the basis of this simple coordination picture one would expect higher Cu moments in the chemically disordered  $\text{Co}_{90}\text{Cu}_{10}$  alloy, where on the average each Cu atom has 10.8 nearest Co neighbors. Hybridization between Cu and Co, and Cu and Fe, however, has to be regarded as two different things because of the different electronic structure of Fe and Co, and may not directly be compared. Furthermore, the electronic structure in an ordered alloy will exhibit significant deviations from that of a disordered alloy due to the chemical periodicity (cf. Sec. III). We conclude that all these effects cancel approximately out, leading to the comparable Cu induced  $3d$  spin moments of FeCu and  $\text{Co}_{90}\text{Cu}_{10}$ .

Theoretically calculated induced moments for the Cu interface layer in Fe/Cu multilayers [ $0.05\text{--}0.07 \mu_B$  (Refs. 21, 22, and 24)] and for Cu in a layered FeCu alloy [ $0.08 \mu_B$  (Ref. 24)] are somewhat lower than our result for the FeCu alloy. As already discussed in the previous section, we attribute this deviation to details of the film structure, and in particular to the vertical atomic distance between the Fe and Cu layers, the exact knowledge of which is crucial for the theoretical description of the magnetic properties of FeCu/Cu(001).

The values obtained from our XMCD data for the spin moments of Fe and Cu (cf. Table I) suggest that about 6% of the magnetization of the FeCu alloy films comes from Cu. It has to be kept in mind, however, that XMCD at the  $L_{2,3}$  edges of Cu and Fe essentially probes only the  $3d$  spin and orbital moments. Whereas for the  $3d$  ferromagnets the total magnetization is predominantly caused by  $d$  states, this is not necessarily true for induced Cu moments. Complementary measurements at the Cu  $K$  edge of Co/Cu and Fe/Cu multilayers, which probe the  $4p$  magnetization, showed a considerable induced Cu  $4p$  moment, which is aligned antiparallel to the Co and Fe magnetization.<sup>20</sup> Comparison to the Co  $4p$  moment gave an estimate of  $-0.03 \mu_B$  for the induced Cu  $p$  moment, which was found to extend well beyond the interface region and into the Cu layers.<sup>20</sup> The results from Fe/Cu multilayers were not as conclusive, but indications for a negative  $4p$  moment like in Co/Cu were also observed.<sup>20</sup> The Cu  $p$  moments therefore are of the same order of magnitude as the  $d$  moments, but of opposite sign. This is also supported by the theoretical results of Refs. 18 and 23. The Cu contribution to the total magnetic moment may thus be significantly smaller than the  $d$  moment. This has to be considered before drawing conclusions from our present data concerning the induced magnetism of Cu in FeCu.



## V. SUMMARY

Epitaxial alloy ultrathin films of the otherwise immiscible elements Fe and Cu were prepared by pulsed-laser deposition on Cu(001) in the ordered  $L1_0$  phase. Electronic properties were studied by spin-resolved valence-band photoemission in normal electron emission. The dispersion of Fe-type majority bands along the  $\Delta$  axis indicates the presence of bands which are a consequence of the reduced size of the alloy Brillouin zone perpendicular to the film plane. This reflects the doubling of the unit cell in the ordered alloy, and indicates the influence of the chemical order on the electronic properties, as well as the hybridization between Fe- and Cu-like bands. X-ray circular magnetic dichroism in  $L_{2,3}$  absorption gave evidence for a ferromagnetic behavior of Fe with moments similar to those of a 3.5 ML Fe/5 ML Co/Cu(001) film. The Fe orbital moments were found to be strongly enhanced in FeCu with respect to pure Fe with an orbital to spin moment ratio of  $\approx 0.12$ . This may be seen as

a hint towards a strong in-plane magnetocrystalline anisotropy. From measurements at the Cu  $L_{2,3}$  edge Cu induced  $d$  moments of  $\approx 0.11 \mu_B$  were found, probably linked to the increase in the number of Cu  $3d$  holes also seen in the XMCD spectra. The enhancement of the Fe orbital moments and the induced Cu moments are attributed to modifications in the FeCu electronic structure due to hybridization between Fe- and Cu-derived states, the reduced symmetry along the surface normal, and the altered dimensionality in the layered alloy films.

## ACKNOWLEDGMENTS

We thank B. Zada for her expert technical support, and the BESSY staff for general support during the beam times. Funding by the German minister of Education, Science, Research, and Technology (BMBF) under Contract No. 05 621EFA 0 is gratefully acknowledged. M.S. thanks the European Union for a stipend.

\*Present address: National Taiwan University, Department of Physics, Taipei, Taiwan.

<sup>1</sup>R. J. Hawkins and J. M. Sanchez, *J. Phys. F* **18**, 767 (1988); J. Kudrnovský, I. Turek, A. Pasturel, R. Tetot, V. Drchal, and P. Weinberger, *Phys. Rev. B* **50**, 9603 (1994); I. A. Abrikosov, P. James, O. Eriksson, P. Söderlind, A. V. Ruban, H. L. Skriver, and B. Johansson, *ibid.* **54**, 3380 (1996).

<sup>2</sup>T. Sato, T. Miyahara, and T. Miyazaki, *J. Magn. Magn. Mater.* **136**, 73 (1994).

<sup>3</sup>*Ultrathin Magnetic Structures*, edited by J. A. C. Bland and B. Heinrich (Springer-Verlag, Berlin, 1994), Vol. 1.

<sup>4</sup>To provide comprehensive references of the system Fe/Cu(100) is beyond the scope of this paper; the interested reader is referred to the references listed in M. T. Kief and W. F. Egelhoff, Jr., *Phys. Rev. B* **47**, 10 785 (1993); S. Müller, P. Bayer, C. Reischl, K. Heinz, B. Feldmann, H. Zillgen, and M. Wuttig, *Phys. Rev. Lett.* **74**, 765 (1995); R. Lorenz and J. Hafner, *Phys. Rev. B* **54**, 15 937 (1996).

<sup>5</sup>M. Zharnikov, A. Dittschar, W. Kuch, K. Meinel, C. M. Schneider, and J. Kirschner, *Thin Solid Films* **275**, 262 (1996).

<sup>6</sup>F. O. Schumann, S. Z. Wu, G. J. Mankey, and R. F. Willis, *J. Appl. Phys.* **79**, 5635 (1996); *Phys. Rev. B* **56**, 2668 (1997); F. O. Schumann, S. Z. Wu, and R. F. Willis, *J. Appl. Phys.* **81**, 3898 (1997).

<sup>7</sup>A. Dittschar, M. Zharnikov, W. Kuch, M.-T. Lin, C. M. Schneider, and J. Kirschner, *Phys. Rev. B* **57**, R3209 (1998).

<sup>8</sup>V. G. Harris, K. M. Kemner, B. N. Das, N. C. Koon, A. E. Ehrlich, J. P. Kirkland, J. C. Woicik, P. Crespo, A. Hernando, and A. García Escorial, *Phys. Rev. B* **54**, 6929 (1996); J. Eckert, J. C. Holzer, C. E. Krill III, and W. L. Johnson, *J. Mater. Res.* **7**, 1980 (1992).

<sup>9</sup>A. R. Yavari, P. J. Desré, and T. Benameur, *Phys. Rev. Lett.* **68**, 2235 (1992).

<sup>10</sup>K. Uenishi, K. F. Kobayashi, S. Nasu, H. Hatano, K. N. Ishihara, and P. H. Shingu, *Z. Metallkd.* **83** (2), 132 (1992).

<sup>11</sup>P. J. Schilling, J.-H. He, J. Cheng, and E. Ma, *Appl. Phys. Lett.* **68**, 767 (1996).

<sup>12</sup>K. Sumiyama, T. Yoshitake, and Y. Nakamura, *Acta Metall.* **33**, 1791 (1983).

<sup>13</sup>C. L. Chien, S. H. Liou, D. Kofalt, W. Yu, T. Egami, and T. R.

McGuire, *Phys. Rev. B* **33**, 3247 (1986).

<sup>14</sup>P. Crespo, A. Hernando, R. Yavari, O. Drbohlav, A. García Escorial, J. M. Barandiarán, and I. Orúe, *Phys. Rev. B* **48**, 7134 (1993).

<sup>15</sup>A. Hernando, P. Crespo, A. García Escorial, and J. M. Barandiarán, *Phys. Rev. Lett.* **70**, 3521 (1993); A. R. Yavari, *ibid.* **70**, 3522 (1993).

<sup>16</sup>P. A. Serena and N. García, *Phys. Rev. B* **50**, 944 (1994).

<sup>17</sup>A. F. Tatarchenko, V. S. Stepanyuk, W. Hergert, P. Rennert, R. Zeller, and P. H. Dederichs, *Phys. Rev. B* **57**, 5213 (1998).

<sup>18</sup>M. G. Samant, J. Stöhr, S. S. P. Parkin, G. A. Held, B. D. Hermsmeier, F. Herman, M. van Schilfgaarde, L.-C. Duda, D. C. Mancini, N. Wassdahl, and R. Nakajima, *Phys. Rev. Lett.* **72**, 1112 (1994).

<sup>19</sup>G. A. Held, M. G. Samant, J. Stöhr, S. S. P. Parkin, B. D. Hermsmeier, M. van Schilfgaarde, and R. Nakajima, *Z. Phys. B* **100**, 335 (1996).

<sup>20</sup>S. Pizzini, A. Fontaine, C. Giorgetti, E. Dartyge, J.-F. Bobo, M. Piecuch, and F. Baudelet, *Phys. Rev. Lett.* **74**, 1470 (1995).

<sup>21</sup>G. Y. Guo, H. Ebert, W. M. Temmerman, and P. J. Durham, *Phys. Rev. B* **50**, 3861 (1994).

<sup>22</sup>O. Hjortstam, J. Trygg, J. M. Wills, B. Johansson, and O. Eriksson, *Phys. Rev. B* **53**, 9204 (1996).

<sup>23</sup>R. Wu and A. J. Freeman, *J. Appl. Phys.* **79**, 6500 (1996).

<sup>24</sup>Y. Zhou, L. Zhong, W. Zhang, and D.-S. Wang, *J. Appl. Phys.* **81**, 4472 (1997).

<sup>25</sup>S. Sundar Manoharan, J. Shen, H. Jenniches, M. Klaua, and J. Kirschner, *J. Appl. Phys.* **81**, 3768 (1997).

<sup>26</sup>S. Sundar Manoharan, M. Klaua, J. Shen, J. Barthel, H. Jenniches, and J. Kirschner, preceding paper, *Phys. Rev. B* **58**, 8549 (1998).

<sup>27</sup>K. Takanashi, S. Mitani, M. Sano, H. Fujimori, H. Nakajima, and A. Osawa, *Appl. Phys. Lett.* **67**, 1016 (1995); S. Mitani, K. Takanashi, H. Nakajima, K. Sato, R. Schreiber, P. Grünberg, and H. Fujimori, *J. Magn. Magn. Mater.* **156**, 7 (1996).

<sup>28</sup>J. Giergiel, J. Shen, J. Woltersdorf, A. Kirilyuk, and J. Kirschner, *Phys. Rev. B* **52**, 8528 (1995).

<sup>29</sup>C. M. Schneider and J. Kirschner, *Crit. Rev. Solid State Mater. Sci.* **20**, 179 (1995).

<sup>30</sup>M. Zharnikov, A. Dittschar, W. Kuch, C. M. Schneider, and J.

- Kirschner, J. Magn. Magn. Mater. **165**, 250 (1997).
- <sup>31</sup>J. L. Erskine and E. A. Stern, Phys. Rev. B **12**, 5016 (1975); G. Schütz, W. Wagner, W. Wilhelm, P. Kienle, R. Zeller, R. Frahm, and G. Materlik, Phys. Rev. Lett. **58**, 737 (1987).
- <sup>32</sup>B. T. Thole, P. Carra, F. Sette, and G. van der Laan, Phys. Rev. Lett. **68**, 1943 (1992).
- <sup>33</sup>P. Carra, B. T. Thole, M. Altarelli, and X. Wang, Phys. Rev. Lett. **70**, 694 (1993).
- <sup>34</sup>R. Wu and A. J. Freeman, Phys. Rev. Lett. **73**, 1994 (1994).
- <sup>35</sup>W. L. O'Brien, B. P. Tonner, G. R. Harp, and S. S. P. Parkin, J. Appl. Phys. **76**, 6462 (1994); D. Rioux, B. Allen, H. Höchst, D. Zhao, and D. L. Huber, Phys. Rev. B **56**, 753 (1997).
- <sup>36</sup>C. T. Chen, Y. U. Idzerda, H.-J. Lin, N. V. Smith, G. Meigs, E. Chaban, G. H. Ho, E. Pellegrin, and F. Sette, Phys. Rev. Lett. **75**, 152 (1995).
- <sup>37</sup>Y. U. Idzerda, C. T. Chen, H.-J. Lin, H. Tjeng, and G. Meigs, Physica B **208–209**, 746 (1995).
- <sup>38</sup>J. Vogel and M. Sacchi, Phys. Rev. B **49**, 3230 (1994).
- <sup>39</sup>X. Le Cann, C. Boeglin, B. Carrière, and K. Hricovini, Phys. Rev. B **54**, 373 (1996).
- <sup>40</sup>J. Hunter Dunn, D. Arvanitis, and N. Mårtensson, Phys. Rev. B **54**, R11157 (1996).
- <sup>41</sup>J. Stöhr, J. Electron Spectrosc. Relat. Phenom. **75**, 253 (1995).
- <sup>42</sup>F. Schäfers, W. Peatman, A. Eyers, C. Heckenkamp, G. Schönhense, and U. Heinzmann, Rev. Sci. Instrum. **57**, 1032 (1986).
- <sup>43</sup>C. M. Schneider, J. J. de Miguel, P. Bressler, P. Schuster, R. Miranda, and J. Kirschner, J. Electron Spectrosc. Relat. Phenom. **51**, 263 (1990).
- <sup>44</sup>H. Petersen, M. Willmann, F. Schäfers, and W. Gudat, Nucl. Instrum. Methods Phys. Res. A **333**, 594 (1993); H. Petersen, C. Jung, C. Hellwig, W. B. Peatman, and W. Gudat, Rev. Sci. Instrum. **66**, 1 (1995).
- <sup>45</sup>T. Böske, W. Clemens, C. Carbone, and W. Eberhardt, Phys. Rev. B **49**, 4003 (1994).
- <sup>46</sup>J. Hunter Dunn, D. Arvanitis, N. Mårtensson, M. Tischer, F. May, M. Russo, and K. Baberschke, J. Phys.: Condens. Matter **7**, 1111 (1995).
- <sup>47</sup>W. Kuch, M.-T. Lin, K. Meinel, C. M. Schneider, J. Noffke, and J. Kirschner, Phys. Rev. B **51**, 12 627 (1995).
- <sup>48</sup>M. Podgórný, J. Magn. Magn. Mater. **78**, 352 (1989).
- <sup>49</sup>Y. Zhou, W. Zhang, L. Zhong, X. Nie, and D.-S. Wang, J. Magn. Magn. Mater. **167**, 136 (1997).
- <sup>50</sup>H. Eckardt, L. Fritsche, and J. Noffke, J. Phys. F **14**, 97 (1984).
- <sup>51</sup>J. G. Tobin, G. D. Waddill, and D. P. Pappas, Phys. Rev. Lett. **68**, 3642 (1992).
- <sup>52</sup>D. E. Fowler and J. V. Barth, Phys. Rev. B **53**, 5563 (1996).
- <sup>53</sup>W. L. O'Brien and B. P. Tonner, Phys. Rev. B **52**, 15 332 (1995); J. Appl. Phys. **79**, 5629 (1996); E. J. Escorcia-Aparicio, R. K. Kawakami, and Z. Q. Qui, *ibid.* **79**, 4964 (1996).
- <sup>54</sup>J. Stöhr and H. König, Phys. Rev. Lett. **75**, 3748 (1995).
- <sup>55</sup>B. D. Cullity, *Introduction to Magnetic Materials* (Addison-Wesley, Reading, MA, 1972).
- <sup>56</sup>M. Tischer, O. Hjortstam, D. Arvanitis, J. Hunter Dunn, F. May, K. Baberschke, J. Trygg, J. M. Wills, B. Johansson, and O. Eriksson, Phys. Rev. Lett. **75**, 1602 (1995).
- <sup>57</sup>D. Weller, Y. Wu, J. Stöhr, M. G. Samant, B. D. Hermsmeier, and C. Chappert, Phys. Rev. B **49**, 12 888 (1994).
- <sup>58</sup>Y. Wu, J. Stöhr, B. D. Hermsmeier, M. G. Samant, and D. Weller, Phys. Rev. Lett. **69**, 2307 (1992).
- <sup>59</sup>O. Eriksson, L. Nordström, A. Pohl, L. Severin, A. M. Boring, and B. Johansson, Phys. Rev. B **41**, 11 807 (1990); H. Ebert, R. Zeller, B. Drittler, and P. H. Dederichs, J. Appl. Phys. **67**, 4576 (1990).
- <sup>60</sup>P. Bruno, Phys. Rev. B **39**, 865 (1989).
- <sup>61</sup>D. Weller, J. Stöhr, R. Nakajima, A. Carl, M. G. Samant, C. Chappert, R. Mégy, P. Beauvillain, P. Veillet, and G. A. Held, Phys. Rev. Lett. **75**, 3752 (1995).
- <sup>62</sup>H. A. Dürr, G. van der Laan, and B. T. Thole, Phys. Rev. Lett. **76**, 3464 (1996); H. A. Dürr and G. van der Laan, Phys. Rev. B **54**, R760 (1996); J. Appl. Phys. **81**, 5355 (1997).
- <sup>63</sup>Xingyu Gao, M. Salvietti, W. Kuch, C. M. Schneider, and J. Kirschner (unpublished).
- <sup>64</sup>H. A. Dürr, G. Y. Guo, G. van der Laan, J. Lee, G. Lauhoff, and J. A. C. Bland, Science **277**, 213 (1997).
- <sup>65</sup>G. Y. Guo, W. M. Temmerman, and H. Ebert, J. Phys.: Condens. Matter **3**, 8205 (1991).
- <sup>66</sup>B. Újfalussy, L. Szunyogh, and P. Weinberger, Phys. Rev. B **54**, 9883 (1996).
- <sup>67</sup>R. Lorenz and J. Hafner, Phys. Rev. B **54**, 15 937 (1996).
- <sup>68</sup>J. Shen, H. Jenniches, Ch. V. Mohan, J. Barthel, M. Klaua, P. Ohresser, and J. Kirschner, Europhys. Lett. (to be published).
- <sup>69</sup>H. Ebert, J. Stöhr, S. S. P. Parkin, M. Samant, and A. Nilsson, Phys. Rev. B **53**, 16 067 (1996).